suggests the existence of plural species of montmorillonite.

These montmorillonite and chlorite do not form mixed layer minerals.

From the above results, we may presume the character of this area's sediments as follows:

From the species of plagioclase and the existence of pyroxene, amphibole and olivine, this area's sediments are mainly minerals basically composed of intermediate or basic igneous rock having sedimented as clastics. Furthermore, the fact that the quantity of clay minerals is small suggests that the alteration is not so advanced. The chlorite and montmorillonite - the clay minerals identified only a small amount - are minerals altered from the above-mentioned mafic minerals and it is hardly conceivable that they are the products of hydrothermal activity or diagenesis.

3) Statistical Analyses

Statistical analyses including multivariate analysis were conducted on 139 samples of sediments collected from the 21 sampling points. Variates subjected to the analyses were mainly the analytical components of chemical analysis.

The analytical software applied to the analysis of variance-covariance matrix of the principal components was ARTHUR (a software of Infometrix, U.S.A.). SPSS/PC (Statistical Package for the Social Sciences / Personal Computer version, a software of SPSS, U.S.A.) was applied to all the analytical processing except for the above.

As for the analytical values that are above the detection limit or below the detection limit in the variates'values of chemical analysis, twice of the values of the detection limit were applied to the former and the half of the values of the detection limit were applied to the latter for the sake of convenience. As for the components which were converted to logarithms, we adopted a notational system as follows; i.e. in case of the SiO_2, we described it as $logSiO_2$ or SiO_2 (log%)

Monovariate analysis was conducted before the multivariate analysis so as to find out the distributed range of the individual variate. The existence of "erratic values" that might disturb the statistical calculation was concluded as negative, so the obtained values were not processed except forthe proceeding of values mentioned above.

<Monovariate Analysis>

The maximum value, minimum value, mean value and standard deviation of each component are shown in Table 4-3-3-1. The mean values and standard deviations were calculated after the analytical values were converted into logarithmic values because each component was concluded from the cumulative frequency distribution map as showing roughly the logarithmic normal distribution. As for the mean values, the logarithmic values of the calculation results were converted back to their original unit. The standard deviations are shown as coefficients against the mean values in the case of $+1\sigma$.

Threshold values were determined from each component's cumulative frequency distribution map and each component's "anormalous value" was shown in its plan view and sectional view. Plan views and sectional views of Boström's Chemical indexes such as Al/Al+Fe+Mn and Fe+Mn/Al, which show the strength of hydrothermal activities, were also drawn. Al/Al+Fe+Mn values of the samples collected from the seafloor surface layers of each sampling point are shown in Fig. 4-3-3-1. Obviously high anormalous values exist at 93SRGC01 and 93SRGC04 in the southwestern part of the survey area. But anormalous values are not identified in the vicinity of the seamounts located in the northeastern part of the survey area from where ore minerals were collected.

Sectional views of each component and depths-components scatter diagrams of each sample were dorawn to discuss the depthwise variation of the chemical component content of each sampling point. Also, the samples were classified into two groups of the brown series (10YR and 2.5YR) and the olive series (5Y) so as to conduct the t-test on these groups of each component. The results of which are shown in Table 4-3-3-2. Most of the brown series samples locate at the upper part of the cores and the olive series samples locate at the lower part of the cores. Accordingly, we can presume that the difference of the chemical component content between the two groups not only shows the defference of color tones but also the difference of chemical environments in which those samples were put. Components/elements significantly rich in the brown series samples are MnO, CaO, CO_2, LOI, Pb, Mn, As and Sr. Which indicates that the brown series samples were relatively in an oxidized environment and are samples rich in foraminiferous fossils. Components/elements significantly rich in the olive series samples as compared with the brown series samples are SiO_2, Al_2O_3, FeO, Na_2O, K_2O, Ag, Hg and Li. Which indicates that the olive series samples were relatively in a reducing environment and are samples poor in foraminiferous fossils

Table 4-3-3-1 Mean, standard deviation, minimum and maximum of chemical component

Entire population

Component	Geometric mean	σ*1	Minimum	Maximum	Unit
SiO2	33.458	1.328	17.18	62.40	%
TiO2	0.445	1.312	0.22	0.79	%
Al2O3	10.399	1.361	1.64	16.94	%
Fe2O3	3.875	1.278	1.76	6.64	%
FeO	1.052	1.961	0.13	4.38	%
MnO	0.164	1.705	0.06	1.40	%
MgO	2.674	1.381	1.18	5.86	%
CaO	19.262	1.481	6.18	35.78	%
BaO	0.0419	1.4044	0.013	0.074	%
Na2O	3.182	1.145	2.19	4.26	%
K2O	1.061	1.363	0.49	3.36	%
P2O5	0.185	1.335	0.09	0.37	%
CO2	10.43	2.32	0.1	27.2	%
LOI	18.285	1.726	1.32	33.29	%
Ag	0.016	2.092	0.01	0.22	ppm
Cu	64.49	1.39	24.0	130.5	ppm
Pb	5.93	1.65	0.5	15.5	ppm
Zn	52.3	1.3	17	109	ppm
Mn	1177.6	1.8	470	20000	ppm
S	0.0688	1.3864	0.026	0.801	%
Cd	0.08	1.59	0.05	0.5	ppm
Ni	34.7	1.4	7	106	ppm
Co	15.8	1.4	4	30	ppm
As	3.15	1.68	0.4	15.0	ppm
Sb	0.11	1.46	0.1	1.0	ppm
Hg	68.9	1.4	40	170	ppb
Ba	345.2	1.4	120	600	ppm
Sr	701.8	1.3	270	1020	ppm
Cl	18151.0	1.4	1600	20000	ppm
P	820.2	1.2	470	1460	ppm
SO4	0.1263	2.7868	0.005	0.428	%
Cr	53.1	1.4	10	133	ppm
V	136.6	1.4	60	340	ppm
Tl	0.35	1.66	0.25	2.0	ppm
B	31.6	1.5	5	55	ppm
Li	12.4	1.4	4	25	ppm
Rb	15.4	1.6	2.5	50	ppm
U	0.49	1.93	0.1	3.6	ppm

*1: $\log(\sigma)$ is standard deviation of $\log(X)$,
where X is concentration of each component.

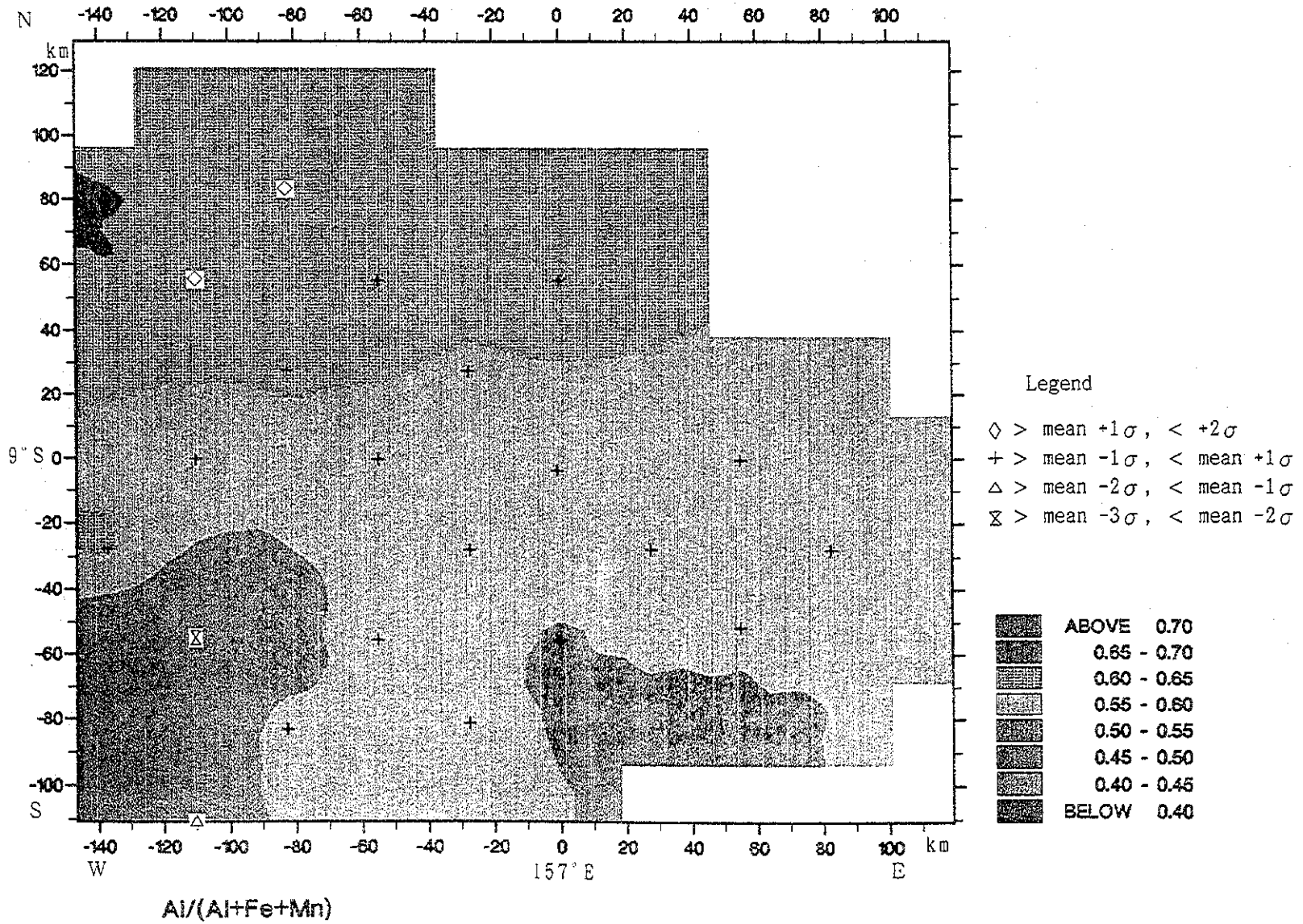

Figure 4-3-3-1 Distribution pattern of ratio of Aℓ/(Aℓ+Fe+Mn)

Table 4-3-3-2 Result of t-test

	Arithmetic Mean (M) and Standard Deviation (σ)		Result of t-test (2-tail)
	Brown M (σ)	Olive M (σ)	
logSiO2	1.4920(.122)	1.5781(.094)	≠**
logTiO2	-.3703(.115)	-.3276(.115)	=
logAl2O3	.9881(.142)	1.0614(.089)	≠**
logFe2O3	.5944(.104)	.5695(.114)	=
logFeO	-.0649(.281)	.1549(.201)	≠**
logMnO	-.7299(.236)	-.9403(.116)	≠**
logMgO	.4051(.124)	.4417(.143)	=
logCaO	1.3282(.152)	1.2160(.171)	≠**
logBaO	-1.3718(.116)	-1.3465(.151)	=
logNa2O	.4930(.058)	.5280(.056)	≠**
logK2O	-.0060(.125)	.1050(.128)	≠**
logP2O5	-.7421(.117)	-.7168(.146)	=
logCO2	1.1020(.287)	.9460(.295)	≠**
logLOI	1.3218(.164)	1.2213(.177)	≠**
logAg	-1.9060(.223)	-1.4953(.339)	≠**
logCu	1.8180(.131)	1.8026(.162)	=
logPb	.8238(.163)	.7170(.212)	≠**
logZn	1.7227(.108)	1.7343(.139)	=
logMn	3.1335(.249)	2.8997(.119)	≠**
logS	-1.1456(.137)	-1.1776(.126)	=
logCd	-1.0669(.182)	-1.0869(.236)	=
logNi	1.5339(.141)	1.5420(.201)	=
logCo	1.2029(.122)	1.1661(.177)	=
logAs	.5700(.172)	.4034(.182)	≠**
logSb	-.9615(.154)	-.9223(.190)	=
logHg	1.8189(.144)	1.8998(.157)	≠**
logBa	2.5411(.112)	2.5708(.143)	=
logSr	2.8715(.090)	2.8191(.092)	≠**
logCl	4.2822(.123)	4.2524(.119)	=
logP	2.9076(.080)	2.9293(.107)	=
logSO4	-.8745(.456)	-.8977(.404)	=
logCr	1.7123(.137)	1.7169(.180)	=
logV	2.1090(.133)	2.1566(.140)	=
logTl	-.4804(.200)	-.3995(.248)	≠*
logB	1.5167(.132)	1.5188(.109)	=
logLi	1.0783(.128)	1.1767(.115)	≠**
logRb	1.1631(.198)	1.2569(.174)	≠*
logU	-.3436(.204)	-.1822(.366)	≠*

* 2-tail prob. <0.05 ** 2-tail prob. <0.01

but rich in clastic minerals. There is no significant difference in the remaining components between the two groups.

The relationships between the content of every two components were shown in correlation scatter diagrams and Pearson's correlation coefficients were also calculated. The variates used are the analytical values that are converted logarithmically. Two-component relations having statistical significance (1-tailed significance < 0.001) and having an absolute value of more than 0.8 in their correlation coefficients are identified between SiO_2-Al_2O_3, TiO_2-MgO, TiO_2-V, MgO-V, CaO-CO_2, CaO-LOI,CaO-Sr, CO_2-Sr, CO_2-LOI, LOI-Sr, Cu-Zn, Ni-Co (the above-mentioned combinations are in the positive correlation) and SiO_2-CaO, SiO_2-CO_2, SiO_2-LOI, Al_2O_3-CaO (the above-mentioned combinations are in the negative correlation).

The relationship to chemical components was examined on quartz, tridymite, plagioclase, pyroxene, halite, calcite, amphibole, montmorillonite and chlorite that are found to be containing in relatively numerous samples by the powder X-ray diffraction test. The abundance of these minerals is indicated by the four ranks as shown below:

Rank 1 (−) : not detected

Rank 2 (±) : diffraction intensity is very weak or the existence of diffraction peak is uncertain

Rank 3 (+) : diffraction intensity is weak

Rank 4 (++) : diffraction intensity is strong

Maximum value, minimum value, mean value and standard deviation of chemical components on each rank were calculated and compared. In order to use the ranks of the above-mentioned minerals for following statistical analysis, the ranks were substituted by values. The relationship between these values and the chemical component values which were converted to logarithms was shown in correlational scatter diagrams for every combination. And Spearman's correlation coefficients, which are the non-parametric rank correlation coefficients, were calculated. The relationship between a mineral and chemical components having statistical significance and having a value of more than +0.4 of correlation coefficient is identified between quartz and Pb·Ba, tridymite and Rb, plagioclase and SiO_2·Al_2O_3·FeO·V, pyroxene and SiO_2·TiO_2·Al_2O_3·FeO·MgO·P_2O_5·Co·P·Cr·V, halite and Ba, calcite and CaO·CO_2·LOI, and chlorite and Cu·Pb·Zn.

<Multivariate Analysis>

Principal component analysis, one of the methods of multivariate analysis, was conducted with the object of analyzing the correlationship among the numerous chemical components analyzed and extracting geochemical (or geological) primary factors that control chemical composition.

Among the 38 chemical components undergone the monovariate analysis, 5 components (i.e. Ag, Cd, Sb, Tl and Cl) were excluded from the subject variates due to the values of exceeding the detection limit or below the detection limit of these five components exceeded 5% among the 139 samples. MnO and BaO were also excluded because they had strong correlation with Mn and Ba respectively. The variates subjected to the principal component analysis, therefore, are SiO_2, TiO_2, Al_2O_3, Fe_2O_3, FeO, MgO, CaO, Na_2O, K_2O, P_2O_5, CO_2 and LOI (their unit is percentage), and Cu, Pb, Zn, Mn, S, Ni, Co, As, Ba, Sr, P, SO_4, Cr, V, B, Li, Rb and U (their unitis ppm) and Hg (its unit is ppb), totaling 31 components. Hereinafter the analytical values expressed by these units are called unit analytical values.

The following treatments were made to the data groups of these 31 variate before the principal component analysis so as to make out 5 data sets for analysis. And the analysis was conducted on each data set.

(i) A correlation matrix in which every unit analytical value was converted to a logarithm and was standardized (the mean value was subtracted from each data and the value was divided by the standard deviation).

(ii) A variance-covariance matrix in which every unit analytical value was used just as it was.

(iii) A variance-covariance matrix in which the percentage unit analytical values were used just as they were, but the ppm and ppb unit analytical values were converted to logarithms.

(iv) A variance-covariance matrix of abundance ratio in which every component was normalized by the abundance of elements of the earth crust (the Clarke numbers).

However, CO_2, LOI and SO_4 were excluded because their abundance of elements were unknown.

(v) A variance-covariance matrix of abundance ratio in which every component was normalized by the sea water dissolved components (Nishimura et al. 1983).

However, Ti, CO_2, LOI and SO_4 were excluded because their sea water dissolved

components were unknown.

Among the results of these principal component analyses, we found that the meaning of most of the variates became indistinct by a very small group of variates which had large standard deviations in the cases of (ii), (iii), (iv) and (v). So we think it meaningless to interpret them except for specific objects. Accordingly, we will interpret the results of the method (i), the scattering of each veriate of which is the most small, in the following.

A factor loading pattern of the method (i) is shown in Table 4-3-3-3. Principal components for analysis were selected from the first 6 principal components having a cumulative contribution rate of more than 80% and an eigenvalue of more than 1. Every principal component was given sense by finding out which variate had the largest factor loading among these six principal components.

On the first principal component, SiO_2, TiO_2, Al_2O_3, Fe_2O_3, FeO, MgO, Na_2O, Ni, Co, P, Cr and V control its factor positively and CaO, CO_2, LOI and Sr control it negatively. From the combination of these components and elements, this principal component is presumed to expressing the amount of clastic minerals in the positive direction and the amount of foraminiferous fossils in the negative direction.

On the second principal component, Cu, Pb, Zn, As, Ba, SO_4, B and Li control its factor positively but factors controlling it negatively are weak. Cu, Pb and Zn are the principal ore elements produced by the already-known submarine hydrothermal activities. As and Ba are also the elements showing high abnormality in hot spring activities. B and Li are also the elememts contained more abundantly in hydrothermal solution erupted from the seafloor than in sea water. Accordingly, this principal component is presumed as indicating a seafloor hydrothermal activity in the positive direction.

On the third principal component, K_2O, Rb and U control positively and Mn control its factor negatively. Such a few factor do not give us any meaning but if we perceive sign and amount of other variates, we can presume that this principal component has possibilites of expressing an acid rock in the positive direction and a basic rock in the negative direction.

On the fourth principal component, S and Hg control its factor positively but the factors controlling it negatively are weak. Besides, SO_4 also controls it positively, so there is a possibility that this principal component indicates a seafloor hydrothermal activity in the positive direction.

Table 4-3-3-3 Factor loading pattern

	PC 1	PC 2	PC 3	PC 4	PC 5	PC 6
logSiO2	[.87161]	-.12400	.39953	.02783	-.12131	-.05244
logTiO2	[.93436]	.23562	-.13755	-.02794	-.03324	.11525
logAl2O3	[.87467]	-.03862	.21085	.01372	-.08740	.00687
logFe2O3	.66494	.55585	-.28201	-.24497	.06713	-.06960
logFeO	[.77242]	-.34089	.02779	.26314	.14094	.28848
logMgO	[.92616]	-.00761	-.27439	.08831	.11342	.06497
logCaO	[-.91356]	.10447	-.27770	-.06796	.08276	.06136
logNa2O	.62132	.35544	.47117	.01739	.03635	-.05744
logK2O	.59919	.18953	.69334	-.11491	-.09070	.08879
logP2O5	.46922	-.11185	.31016	-.32357	.53602	-.21179
logCO2	[-.86629]	.34330	-.02677	-.13651	.07319	.13170
logLOI	[-.82781]	.46962	-.02423	-.04964	.12647	.11755
logCu	.48336	.68841	-.20125	-.04809	.08169	.22579
logPb	-.30649	[.75305]	.00569	-.13272	-.09392	-.06918
logZn	.28694	[.86699]	-.12655	-.07790	-.03723	.24036
logMn	.13905	.37183	-.55527	-.30452	-.34004	-.38153
logS	-.16199	.42106	-.13550	.56340	.28332	-.22013
logNi	.55640	.54711	-.48529	.12537	-.08660	-.00019
logCo	.65419	.28707	-.59188	-.01935	-.09875	.03422
logAs	-.17810	[.70099]	-.12234	-.14362	.32621	-.31343
logHg	-.08736	.42397	.17500	.55656	.20292	-.09203
logBa	-.36651	[.70759]	.32216	.07828	-.29664	-.10911
logSr	[-.83789]	.22743	-.04012	-.24431	.10312	.22893
logP	.65204	.22240	.01676	-.34345	.41490	.19900
logSO4	-.28876	.49136	-.16507	.44917	-.01991	.26136
logCr	.65557	.14848	-.29977	.16739	.01929	-.30026
logV	[.91773]	-.07361	-.30046	.07897	.09794	.05420
logB	-.31740	.59911	.34492	-.16274	.19747	-.03142
logLi	.08490	[.84126]	.31884	.13028	-.17291	.15128
logRb	.49314	.36338	.52750	-.23834	-.24860	.01337
logU	.04281	.32955	.63265	.25303	.03882	-.19188
Eigenvalue	11.73217	6.36085	3.48278	1.64941	1.17671	.94096
Pct of Var	37.8	20.5	11.2	5.3	3.8	3.0
Cumulative Pct of Var	37.8	58.4	69.6	74.9	78.7	81.8

[ ]: factor loading >0.7 or <-0.7
PC:Principal component; Pct of Var:Percent of variability explained
Matrix analyzed by the statistics was correlation matrix of the following componets:
SiO2-LOI(log %), Ag-As & Ba-U(log ppm), Hg(log ppb).

On the fifth principal component, P_2O_5 controls its factor positively but the factors controlling it negatively are weak. As also controls it negatively. There is a possibility that this principal component indicates a seafloor hydrothermal activityin the positive direction because P_2O_5 and As are the components characteristically adsorbing to iron hydroxides.

On the sixth principal component, controlling its factor are weak both in the positive and negative directions. We, therefore, don't know its meaning.

As described above, we can quite clearly interpret the meanings of the first and second principal components but there are a lot of indistinct points in the meanings of the principal components from the third one to the sixth one.

A factor score distribution patten of the first principal component of the samples collected from the seafloor surface layer of each sampling point is shown in Fig. 4-3-3-2 and a factor score distribution pattern of the second principal component is shown in Fig. 4-3-3-3. The factor score of the first principal component is high in the southwestern half of the survey area and low in the northeastern half. It indicates that the samples of the southwestern half of the survey area are rich inforaminiferous fossils and the samples of the northeastern half is rich in clastic minerals. These results were also expected from the microscopic observation of the sedimentary samples conducted on board. Although high factor scores of the second principal component are identified at 93SRGC03 and 93SRGC04 located at the southwestern tip of the survey area but there is no conspicuous difference between it and other samples macroscopically. Furthermore, the factor score of the second principal component is low in the vicinity of the seamount lying in the northeastern part of the survey area from where ore minerals were collected.

Depthwise variations of each principal component's score are shown in cross-section diagrams on each sampling point. Characterictic variations are not identified from them.

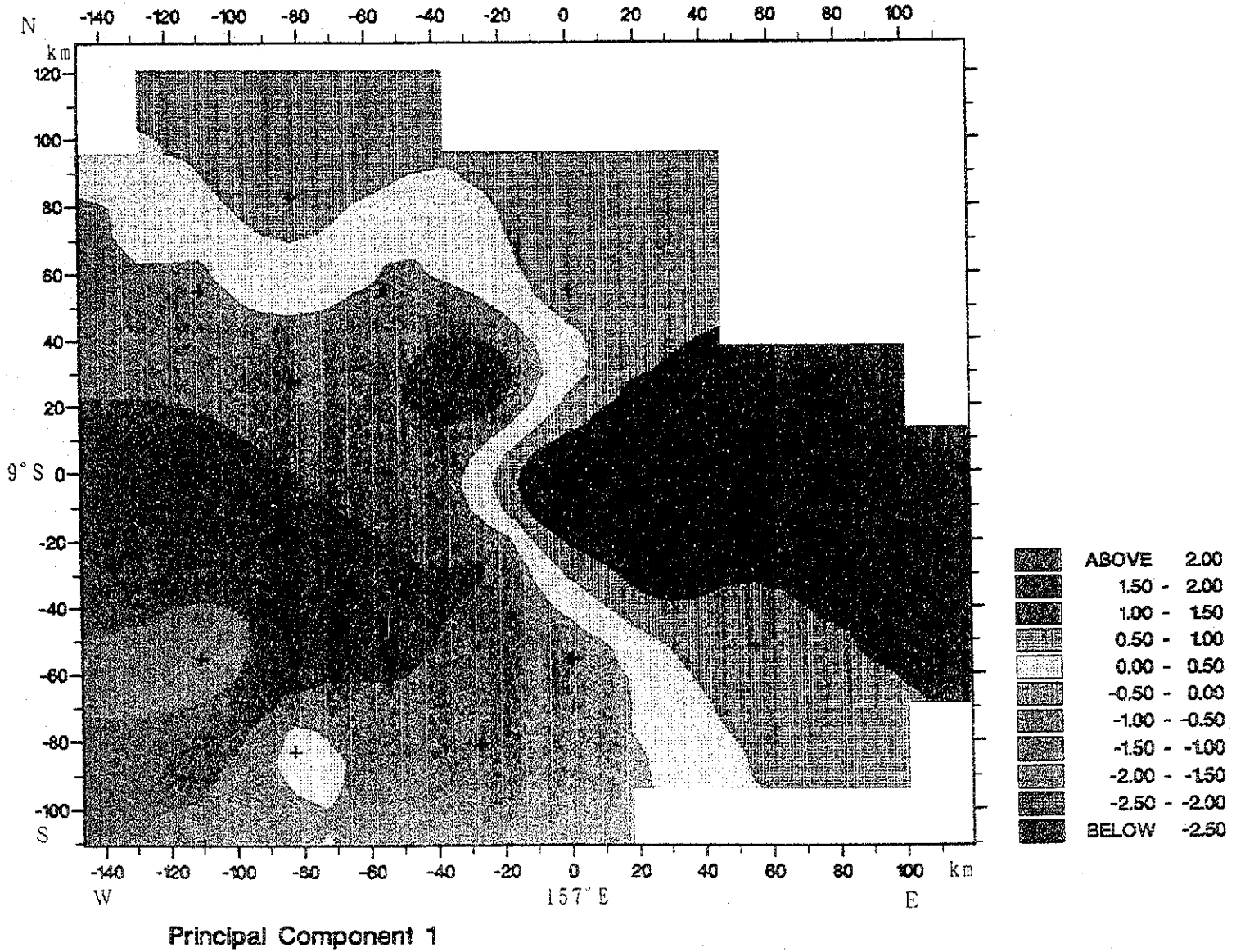

Figure 4-3-3-2 Distribution pattern of the factor score of principal component 1

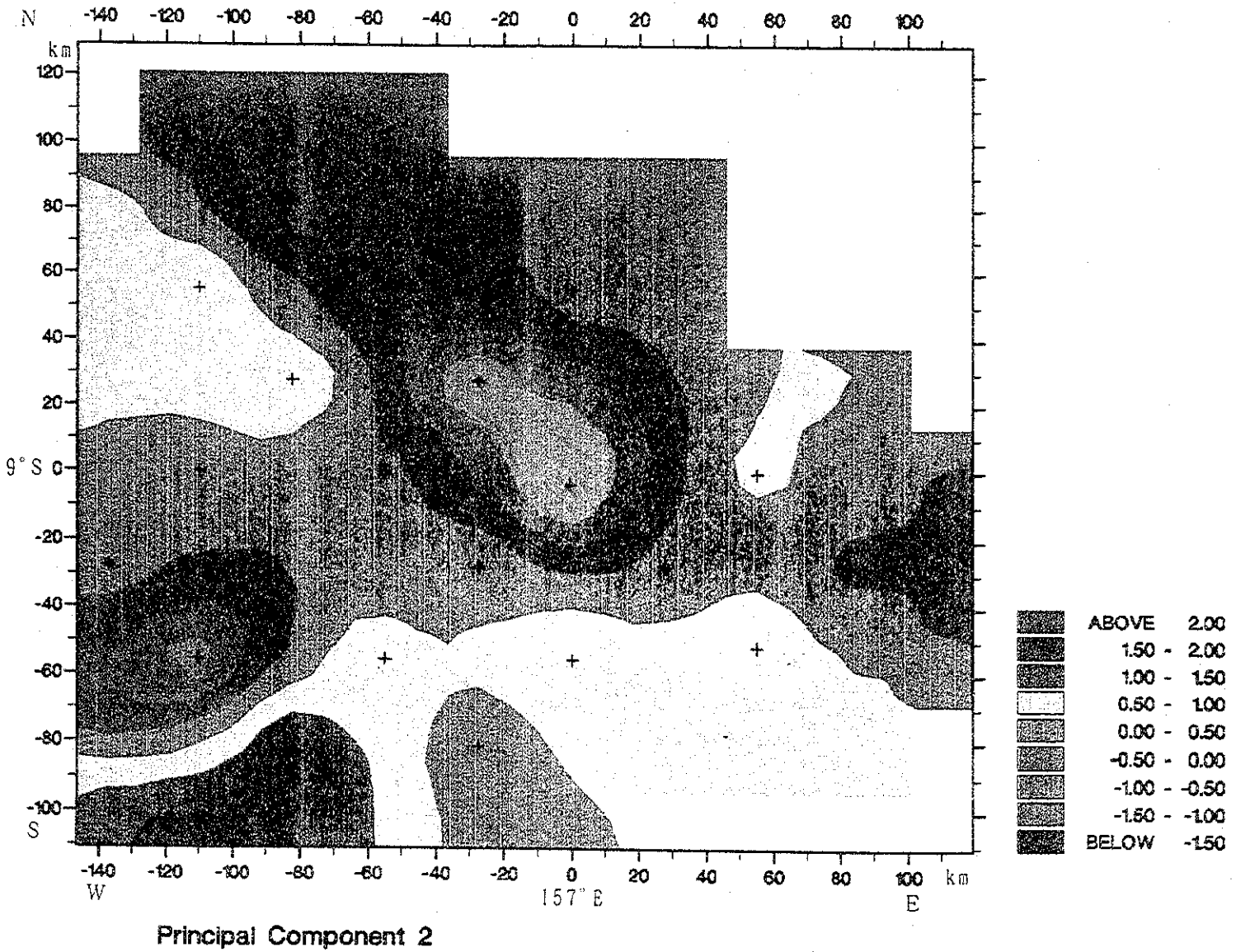

Figure 4-3-3-3 Distribution pattern of the factor score of principal component 2

Chapter 5. Detailed Survey

5-1 Outline

As a result of the past survey made in the western sea area of the Woodlark Basin, a report on hydrothermal activity was made (Binns, R.A. and Wheller, G.E., 1991). But no report on hydrothermal activity has been made to the eastern sea area of the Woodlark Basin. We, therefore, decided to carry out this cruise in this area.

As the existence of submarine hydrothermal deposits was anticipated on the seamounts arranged from north to south on the circumference of the Woodlark Seafloor Spreading Center, identified as a result of the topographic survey and magnetic survey carried out in this sea area, as well as on the Ghizo Ridge, Simbo Ridge, Kana Keoki Seamount and Coleman Seamount, we therefore, carried out the FDC survey at 9 track lines centering around these seamounts. As a result, oxidized alteration was identified at 5 points at 93SFDC03, 3 points at 93SFDC04 and 1 point at 93SFDC07.

Sampling with the CB was made at 12 sampling points at these oxidized alteration zones and the Woodlark Spreading Center (see Annexed Figure 5). And, sampling through the FPG observation was made at 4 sampling points on the Kana Keoki and Coleman Seamounts.

The number of sampling points are indicated by 93 (the latter two figures of the Christian Era) + S (abbreviation of SOPAC) + D (abbreviation of Detail) + CB or PG (the sampling methods: CB represents Chain Bucket and PG represents Power Grab) + serial number in two figures in order of sampling trial. In this fiscal year's survey, the first sampling points are represented by "93SDCB01" for the CB sampling and "93SDPG01" for the PG sampling. The last sampling points for the CB is represented by "93SDCB12", and for the PG by "93SDPG04". During the CB sampling operation, light gray clay and siliceous rock containing a trace of pyrite were collected from the vicinity of the summit of the Kana Keoki Seamount. Rock covered with iron-manganese oxides was collected from other points.

We could not identify hydrothermal activity by the FDC observation. But we have observed oxidation alteration at 9 points.

In this Chapter, we will describe the results of the FDC observation survey and CB sampling, FPG observation and sampling.

5-2 Submarine Geology

1) The Results of the FDC Observation

The seafloor were observed by the FDC, and color photographs were taken and color video tapes were recorded at the seamounts on the SE trending the Ghizo Ridge which links with the Coleman Seamount, the seamounts on the N-S trending Simbo Ridge and seamounts scattered around the northern and southern sides of the E-W trending Woodlark Spreading Center.

The location of each track line is shown in Figure 5-2-1-1 and the photographs of typical seafloor are shown in Figure 5-2-1-2. The results of the FDC survey are shown in Table 5-2-1-1. The results of each track line are as follows:

<Track line 93SFDC01>

The location of the towing line, duration of observation and number of photographs taken are as follows:

Started at	: 22:00 on Sept. 23, 1993 (GMT)
Finished at	: 05:00 on Sept. 24, 1993 (GMT)
Starting point	: 8° 37.91'S·156° 37.75'E
Terminal point	: 8° 42.99'S·156° 44.50'E
Towed azimuth	: 127°
Distance observed	: 8.5 miles
Water depths observed	: between 1,490 m and 2,548 m
Duration of observation	: 7 hours and 00 minutes
Number of photographs taken	: 204 points

The observation was carried out in the azimuth of NW ~ SE parallel to the axial of the Ghizo Ridge. The location of the track line is shown in Annexed Figure 3(1) and the route map is shown in Annexed Figure 4(1).

Sandy ~ muddy sediments are relatively prominent on this track line. The observed ratio between sediments and outcropped rock is roughly 2:1. Sandy ~ muddy sediments assume dark brown. The thickness of the sediments is considered to be thick (estimated from the data of 93SRGC10 as thicker than 2 m) around the margins of the summit, but relatively thin on the slopes where the sediments are distributed over rocks. Pumice and scoria are recognized on the surface of sandy ~ muddy sediments. Ripple marks are recognized on some places.

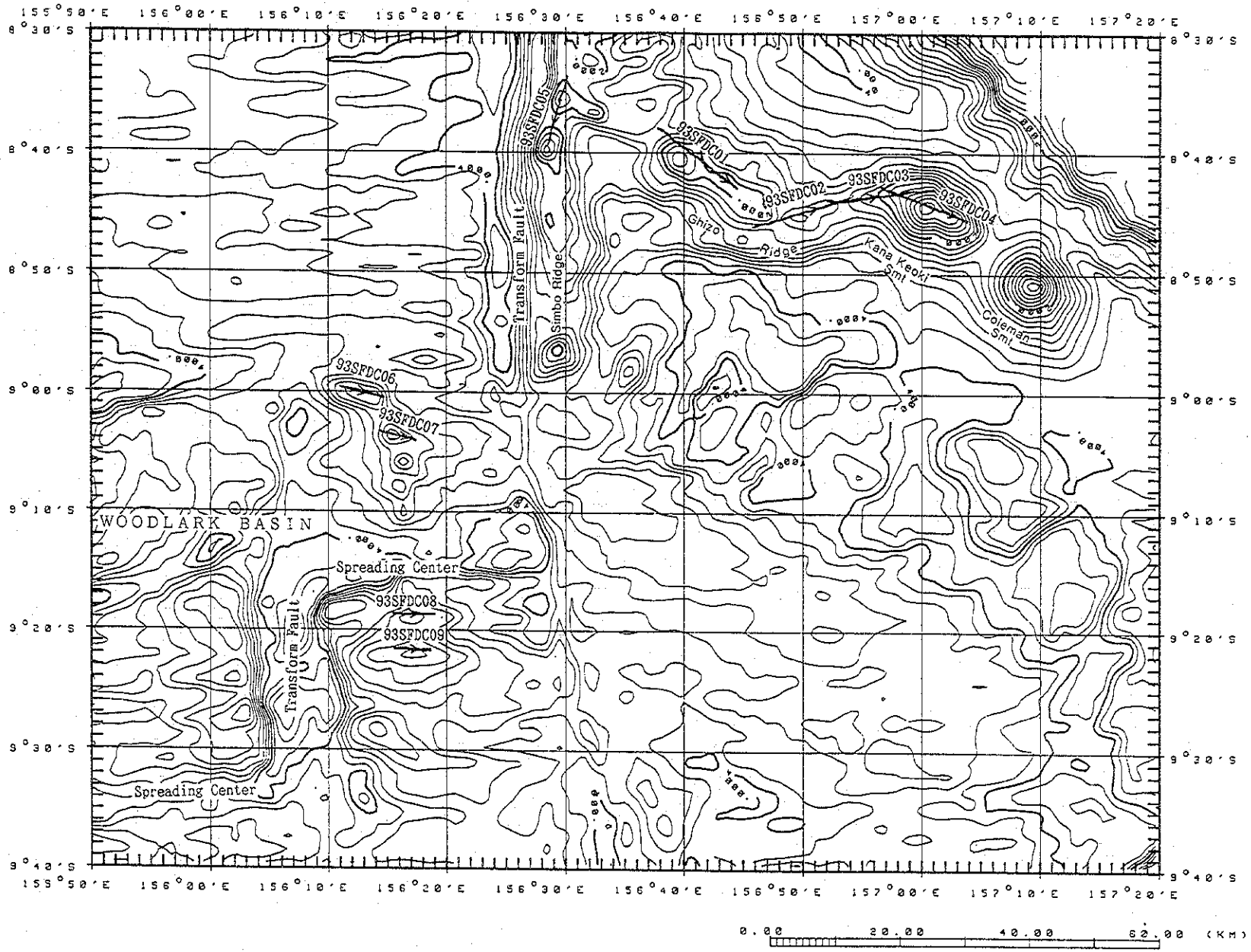

Figure 5-2-1-1 Location Map of FDC Lines (General View)

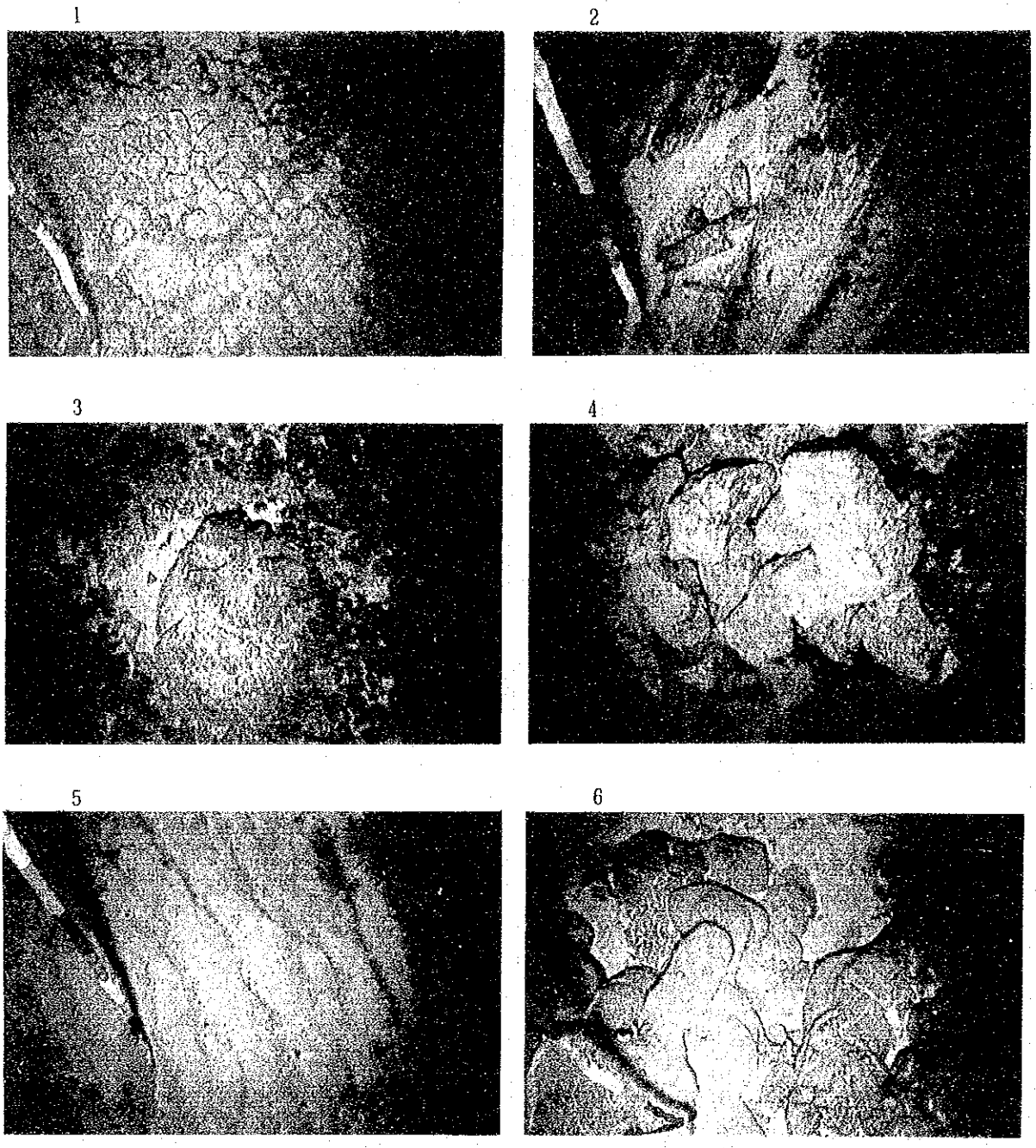

1. Autobrecciated lave Line93SFDC01 (8°41.53'S, 156°42.51'E, water depth2,117m)
2. Sheet lave Line93SFDC02 (8°45.89'S, 156°46.99'E, water depth2,458m)
3. Pillow lave (pillow shape) Line93SFDC05 (8°36.44'S, 156°29.22'E, water depth1,876m)
4. Talus Line93SFDC05 (8°39.26'S, 156°28.53'E, water depth1,664m)
5. Ripple marks Line93SFDC06 (8°59.61'S, 156°11.09'E, water depth2,746m)
6. Pillow lave (tube shape) Line93SFDC06 (8°59.65'S, 156°11.29'E, water depth2,638m)

Figure 5-2-1-2 Seafloor Photographs taken by FDC (1)

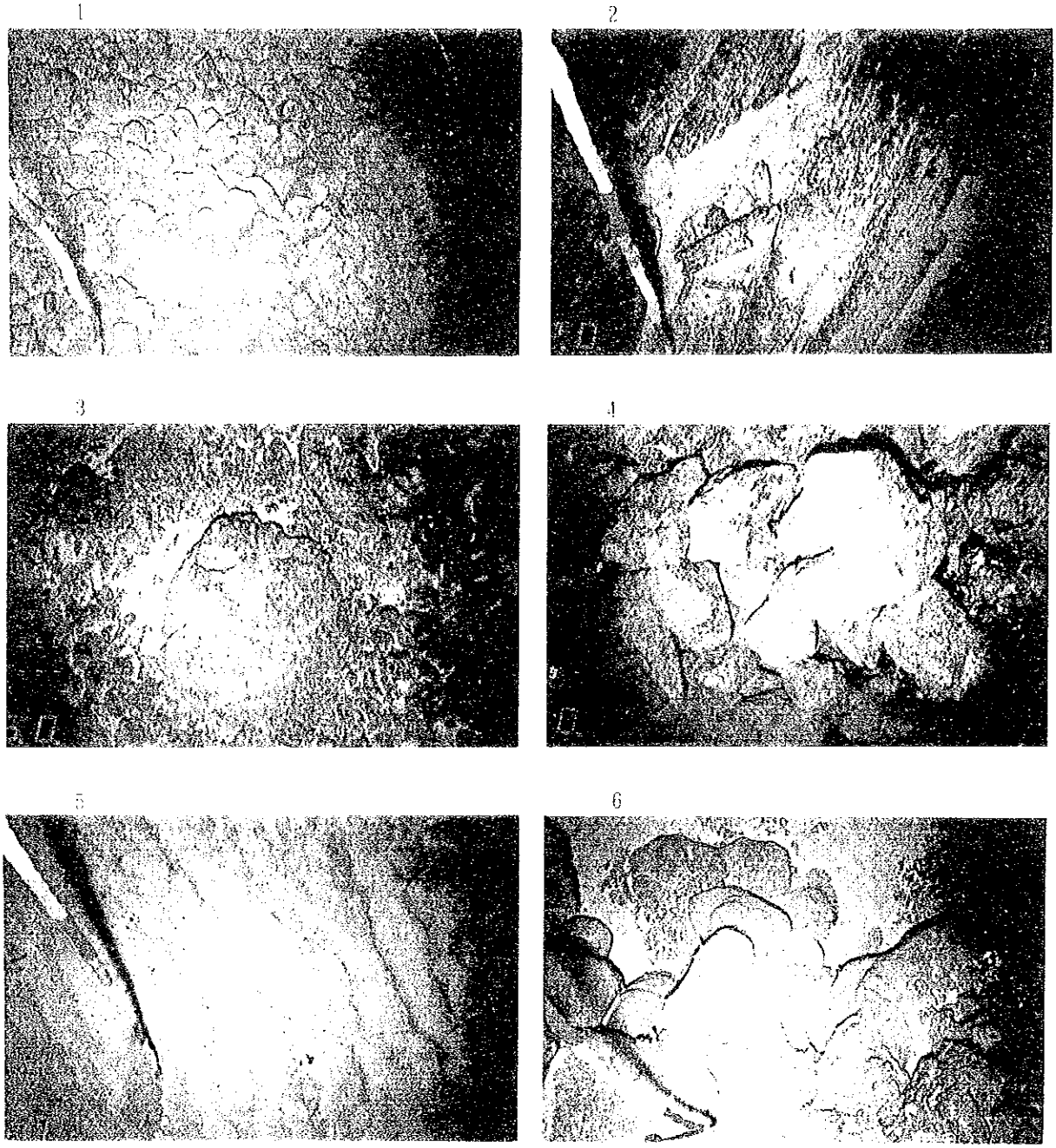

1. Autobrecciated lave　Line93SFDC01 (8°41.53'S, 156°42.51'E, water depth2,117m)
2. Sheet lave　Line93SFDC02 (8°45.89'S, 156°46.99'E, water depth2,458m)
3. Pillow lave (pillow shape)　Line93SFDC05 (8°36.44'S, 156°29.22'E, water depth1,876m)
4. Talus　Line93SFDC05 (8°39.26'S, 156°28.53'E, water depth1,664m)
5. Ripple marks　Line93SFDC06 (8°59.61'S, 156°11.09'E, water depth2,746m)
6. Pillow lave (tube shape)　Line93SFDC06 (8°59.65'S, 156°11.29'E, water depth2,638m)

Figure 5-2-1-2　Seafloor Photographs taken by FDC (1)

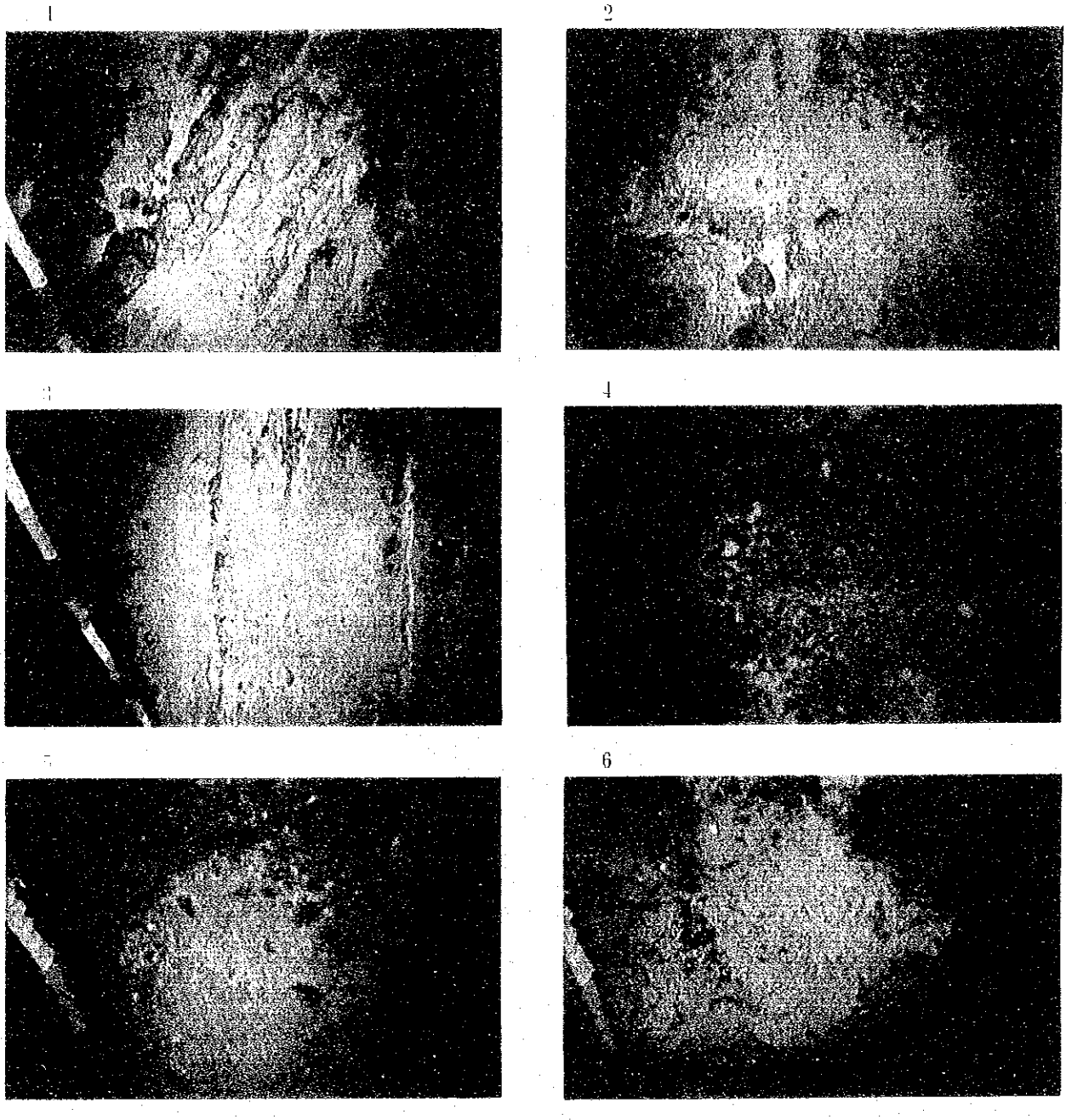

1. white coloured lave.
   Line93SFDC02 (8°45.32'S, 156°48.63'E, water depth2,093m)
2. white coloured lava and brown sediment.
   Line93SFDC02 (8°44.96'S, 156°49.86'E, water depth2,021m)
3. white coloured lava.
   Line93SFDC02 (8°44.96'S, 156°49.87'E, water depth1,022m)
4. brown sediment coloured by pumice.
   Line93SFDC03 (8°43.05'S, 157°00.36'E, water depth1,352m)
5. brown sediment coloured by hydroxide
   Line93SFDC04 (8°44.36'S, 157°00.60'E, water depth 723m)
6. brown sediment coloured by hydroxide
   Line93SFDC04 (8°45.31'S, 157°03.01'E, water depth 775m)

Figure 5-2-1-2 Seafloor Photographs taken by FDC (2)

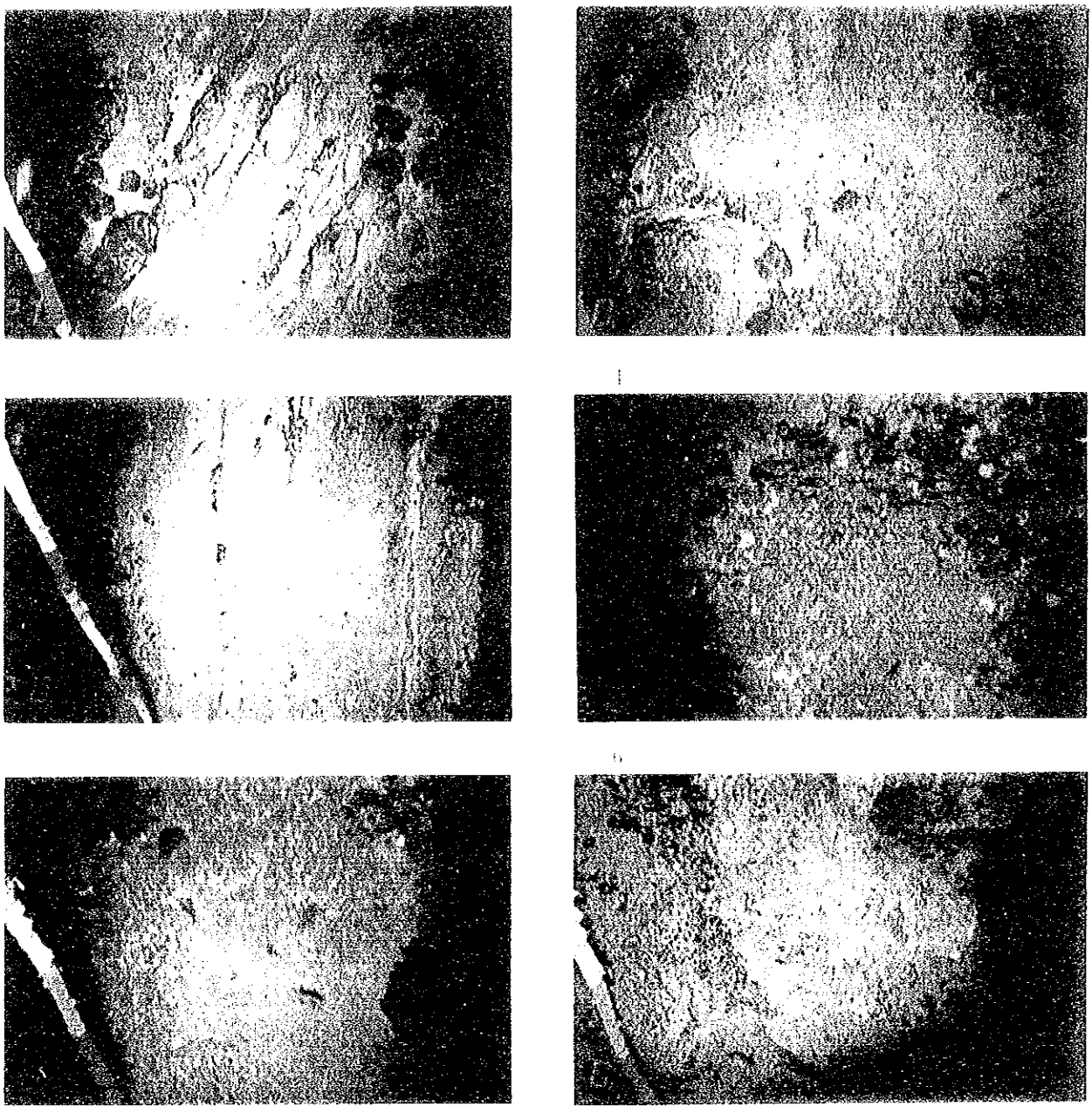

1. white coloured lave.
   Line93SFDC02 (8°45.32'S, 156°48.63'E, water depth2,093m)
2. white coloured lava and brown sediment.
   Line93SFDC02 (8°44.96'S, 156°49.86'E, water depth2,021m)
3. white coloured lava.
   Line93SFDC02 (8°44.96'S, 156°49.87'E, water depth1,022m)
4. brown sediment coloured by pumice.
   Line93SFDC03 (8°43.05'S, 157°00.36'E, water depth1,352m)
5. brown sediment coloured by hydroxide
   Line93SFDC04 (8°44.36'S, 157°00.60'E, water depth 733m)
6. brown sediment coloured by hydroxide
   Line93SFDC04 (8°45.31'S, 157°03.01'E, water depth 775m)

Figure 5-2-1-2 Seafloor Photographs taken by FDC (2)

Table 5-2-1-1 Results of FDC Observation (1)

Date	Track Line No.	(a)Plunbing Time (b)Landing Time (c)Taking-off Time (d)Hauling-up Time	Location Latitude	 Longitude	Depth (m)	Duration of Operation (a)～(d)	Duration of bottom Observation (b)～(c)	Length Observed (mile)	Number of Photos Taken	Details of the Observation
9/23	93SFDC01	Plunbing Time 21:06 Landing Time 22:00	8°37.91′S	156°37.75′E	2,519	8:31	7:00	8.5	204	Observed the western crest of the Ghizo Ridge. Sandy and muddy sediments:outcropping rocks = 2:1. Sandy and muddy sediments are thick at margin of the crest but thin on the slopes. A small amount of pumice and scoria are observed on the sediments. Rocks are mainly composed of autobrecciated lave, but pillow lava and talus are recognized partially. Apparent sign of mineralization are not recognized. Munidopsis sp. are rarely observed.
9/24		Taking-off Time 05:00 Hauling-up Time 05:37	8°42.99′S	156°44.50′E	1,861					
9/24	93SFDC02	Plunbing Time 21:05 Landing Time 22:00	8°46.20′S	156°45.81′E	2,563	8:45	6:59	8.3	241	Observed the eastern crest of the Ghizo Ridge. Sandy and muddy sediments: rocks =1:4. Sandy and muddy sediments are relatively thin. Rocks are mainly composed of autobrecciated lava, but pillow lava and talus are observed partially. Apparent sign of mineralization are not recognized. Such biota as crinoids ,asteroids, holothurians, macrurans and sponges are observed.
9/25		Taking-off Time 04:59 Hauling-up Time 05:50	8°43.73′S	156°53.81′E	2,364					
9/26	93SFDC03	Plunbing Time 20:50 Landing Time 21:34	8°44.06′S	156°52.30′E	2,193	8:07	6:54	8.7	261	Observed the northern flank crest of the Kana Keoki seamount. Sandy and muddy sediments:outcropping rocks 3:1. Sandy and muddy sediments are relatively thin. Rocks are mainly composed of autobrecciated lava, but talus are observed partially. Brown precipitats are devived from oxidates, which are discoverd at five points. Such biotas as crinoids, asteroids, holothurians, macrurans and sponges are observed.
9/27		Taking-off Time 04:28 Hauling-up Time 04:57	8°43.03′S	157°01.03′E	1,178					
9/26	93SFDC04	Plunbing Time 20:55 Landing Time 21:40	8°42.80′S	156°56.58′E	2,113	8:02	6:49	7.7	261	Observed the summit part of the Kana Keoki seamount. Sandy and muddy sediments:rocks =4:1. Sandy and muddy sediments are relatively thin. Rocks are mainly composed of autobrecciated lava, and rippie marks are not recognized on sediments. Dark brown sediments are derived from iron oxidates, which are discovered at three points . A lot of macrurans are observed around the shallower crest.
9/27		Taking-off Time 04:29 Hauling-up Time 04:57	8°45.36′S	157°03.74′E	1,218					
9/27	93SFDC05	Plunbing Time 20:57 Landing Time 21:44	8°33.52′S	156°30.09′E	1,951	5:38	4:10	6.1	127	Observed the seamount of the Shimbo Ridge in the direction of NNE-SSW. Sandy and muddy sediments are relatively thin. Rocks are mainly composed of autobrecciated lava, and talus are prominent on the southern crest. Ripple marks are rarely observed on sediments. Apparent sign of mineralization are not recognized. Such biota as crinoids, asteroids, holothurians, macrurans and sponges are observed.
9/27		Taking-off Time 01:54 Hauling-up Time 02:35	8°39.40′S	156°28.47′E	1,462					

Table 5-2-1-1 Results of FDC Observation (2)

Dat	Track Line N	(a)Plunbing Time (b)Landing Time (c)Taking-off Time (d)Hauling-up Time Time	Location Latitude	 Longitude	Depth (m)	Duration of Operation (a)~(d)	Duration of bottom Observation (b)~(c)	Length Observed (mile)	Number of Photos Taken	Details of the Observation
10/05 10/06	93SFDC06	Plunbing Time 20:33 Landing Time 21:29 Taking-off Time 00:41 Hauling-up Time 01:32	8°59.62'S 9°00.51'S	156°11.00'E 156°14.61'E	2,741 2,445	4:59	3:12	3.5	112	Observed the northern seamount in the direction of W-E, which located in the north of the spreading center. The scope of the sandy and muddy sediments observed are narrow and thin. Rocks with pillow and tube shaped lava is well-developed on the western slopes. Porous and coarse-grained slaggy lava and talus are well-developed from western crest to eastern slopes. Apparent sign of mineralization are not recognized.
10/06 10/06	93SFDC07	Plunbing Time 01:58 Landing Time 02:53 Taking-off Time 05:55 Hauling-up Time 06:49	9°03.39'S 9°04.13'S	156°14.34'E 156°17.29'E	2,911 2,558	4:51	3:02	3.1	104	Observed the southern seamount in the direction of W-E, which located in the north of the spreading center. Sandy and muddy sediments are observed on the crest as well as on the terrace. Sandy and muddy sediments are relatively thin. Rocks are mainly pillow and tube shaped lava, but slaggy lava and talus are recognized locally. Oxidized brown precipitats are discovered at one point.
10/06 10/07	93SFDC08	Plunbing Time 20:56 Landing Time 21:57 Taking-off Time 01:16 Hauling-up Time 02:13	9°18.72'S 9°18.72'S	156°15.51'E 156°18.99'E	3,135 2,767	5:17	3:19	3.1	112	Observed the northern seamount in the direction of W-E, which located in the south of the spreading center. The scope of observable sandy and muddy sediments is narrow. Ripple marks are recognized. Slaggy lava is prominent on western slopes and on the crest. Apparent sigh of mineralization are not recognized. Munidosis sp are observed.
10/07 10/07	93SFDC09	Plunbing Time 02:55 Landing Time 03:47 Taking-off Time 06:41 Hauling-up Time 07:31	9°21.66'S 9°21.68'S	156°15.57'E 156°18.65'E	2,605 2,372	4:36	2:54	3.0	102	Observed the southern seamount in the direction of W-E, which located in the south of the spreading center. The scope of observable sandy and muddy sediments is narrow. Ripple marks are recognized. Talus are recognized in margin of the western crest. Pillow lava is recognized on the crest. Slaggy lava and pillow lava are recognized in the margin of the eastern crest. Apparent sign of mineralization are not recognized.

Notes: Date and time are in GMT. Towing vehicle were calculated from the winch length and water depth by CTD.

Rocks are mainly composed of autobrecciated lava but pillow lava is partially recognized, and talus breccias covering these two kinds of lava are prominent. Large blocks of rock are outcropped from beneath massed pebbles here and there. Joints are recognized in these blocks of rock.

Apparent signs of mineralization are not recognized on this track line.

Living things observed on this track line include echinoderms such as crinoids, ferns, asteroids, echinoids and holothurians, coelenterates such as actiniae, and fishes, shrimps, *Munidopsis sp.* and sponges.

Trace fossils are observed here and there on the surfaces of the sandy ~ muddy sediments.

<Track line 93SFDC02>

The location of the towing line, duration of observation and number of photographs taken are as follows:

Started at	: 22:00 on Sept. 24, 1993 (GMT)
Finished at	: 04:59 on Sept. 25, 1993 (GMT)
Starting point	: 8° 46.20'S·156° 45.81'E
Terminal point	: 8° 43.73'S·156° 53.81'E
Towed azimuth	: 72°
Distance observed	: 8.3 miles
Water depths observed	: between 2,018 m and 2,592 m
Duration of observation	: 6 hours and 59 minutes
Number of photographs taken	: 241 points

The observation was carried out on an eastern area of the track line 93SFDC01 along the axial of the Ghizo Ridge. The location of the track line is shown in Annexed Figure 3(2) and the route map is shown in Annexed Figure 4(2).

Sandy ~ muddy sediments are relatively few on this track line. The observed ratio between sediments and outcropped rock is roughly 1:4. Sandy ~ muddy sediments assume dark brown. Sediments are distributed over rocks. As rocks are often outcropped from beneath the sediments, the thickness of the sediments are considered to be relatively thin. Ripple marks are observed rarely. Rocks are mainly composed of autobrecciated lava but pillow lava and talus breccias are observed partially.

Apparent signs of mineralization are not recognized on this track line but lava, the surface of which is altered and assuming white, and brown precipitates are partly

observed.

Living things observed on this track line include echinoderms such as crinoids, asteroids, echinoids and holothurians, coelenterates such as actiniae, and fishes, shrimps and sponges.

A number of trace fossils are observed on the surfaces of the sandy ～ muddy sediments.

<Track line 93SFDC03>

The location of the towing line, duration of observation and number of photographs taken are as follows:

Started at	: 21:34 on Sept. 25, 1993 (GMT)
Finished at	: 04:28 on Sept. 26, 1993 (GMT)
Starting point	: 8° 44.06'S·156° 52.30'E
Terminal point	: 8° 43.03'S·157° 01.03'E
Towed azimuth	: 82°
Distance observed	: 8.7 miles
Water depths observed	: between 1,177 m and 2,442 m
Duration of observation	: 6 hours and 54 minutes
Number of photographs taken	: 261 points

The observation was carried out on the eastern area of the track line 93SFDC02 which runs along the axis of the Ghizo Ridge until the northward slope of the Kana Keoki Seamount. The location of the track line is shown in Annexed Figure 3(3) and the route map is shown in Annexed Figure 4(3).

Outcropped rock is relatively prominent on this track line. The range with sandy ～ muddy sediments is narrow. The observed ratio between outcropped rock and sediments is roughly 3:1. Sandy ～ muddy sediments assume dark brown. Sediments are distributed over rocks. As rocks are often outcropped from beneath the sediments, the thickness of the sediments are considered to be relatively thin. Ripple marks are not recognized on the surface of sediments. Rocks are mainly composed of autobrecciated lava but talus breccias are observed on the ridge part developed on the northwestern slope of the Kana Keoki Seamount.

Browned precipitates, which are considered to be iron oxides, are recognized intermittently in this track line near at 8° 43.3'S·156° 58.8'E (at the water depth of 1,694 m), 8° 43.2'S·156° 59.1'E (at the water depth of 1,594 m) and 8° 43.0'S

·157° 00.4'E (at the water depth of 1,352 m) as well as at two other points for two to five minutes of the duration of observation (for the distance roughly 60 ~ 150 m).

Living things observed on this track line include echinoderms such as crinoids, asteroids, echinoids and holothurians, coelenterates such as actiniae, and fishes and shrimps.

Trace fossils are observed, though rarely, on the surface of sandy ~ muddy sediments.

<Track line 93SFDC04>

The location of the towing line, duration of observation and number of photographs taken are as follows:

Started at	: 21:40 on Sept. 26, 1993 (GMT)
Finished at	: 04:29 on Sept. 27, 1993 (GMT)
Starting point	: 8° 42.80'S·156° 56.58'E
Terminal point	: 8° 45.56'S·157° 03.74'E
Towed azimuth	: 111°
Distance observed	: 7.7 miles
Water depths observed	: between 670 m and 2,113 m
Duration of observation	: 6 hours and 49 minutes
Number of photographs taken	: 261 points

The observation was carried out in the azimuth of NW-SE from the northwestern slope of the Kana Keoki Seamount, through the crest part up to the southeastern slope. The location of the track line is shown in Annexed Figure 3(4) and the route map is shown in Annexed Figure 4(4).

Outcropped rock is relatively prominent on this track line. Sandy ~ muddy sediments are observed on the terrace part of the southeastern slope. Sediments of black volcanic ashes and scoria are rarely observed. The observed ratio between the former and the latter is roughly 4:1. Sandy ~ muddy sediments assume dark brown. Sediments are distributed over rocks. As rocks are often outcropped from beneath the sediments, the thickness of the sediments are considered to be thin. Ripple marks are not recognized on the surface of sediments. Rocks are mainly composed of underwater autobrecciated lava.

Precipitates appeared to be iron oxides are recognized intermittently in the vicinity of the crests located on this track line at 8° 44.4'S·157° 00.6'E (at the

water depth of 726 m), 8° 44.6'S·157° 00.9'E (at the depth of 689 m) and 8° 44.7'S ·157° 01.5'E (at the depth of 951 m) for two to five minutes (for the distance roughly 60 ～ 150 m).

Living things observed on this track line include echinoderms such as crinoids, asteroids, echinoids and holothurians, coelenterates such as actiniae, and fishes and shrimps. A large number of shrimps are observed in the vicinity of the crests at shallow water.

Trace fossils are observed on the surfaces of sandy ～ muddy sediments.

<Track line 93SFDC05>

The location of the towing line, duration of observation and number of photographs taken are as follows:

Started at	: 21:44 on Sept. 27, 1993 (GMT)
Finished at	: 01:54 on Sept. 28, 1993 (GMT)
Starting point	: 8° 33.52'S·156° 30.09'E
Terminal point	: 8° 39.40'S·157° 28.47'E
Towed azimuth	: 195°
Distance observed	: 6.1 miles
Water depths observed	: between 1,335 m and 1,952 m
Duration of observation	: 4 hours and 10 minutes
Number of photographs taken	: 127 points

The observation was carried out in the azimuth of NNE ～ SSW roughly along the Simbo Ridge crests. The location of the track line is shown in Annexed Figure 3(5) and the route map is shown in Annexed Figure 4(5).

Outcropped rock is prominent on this track line and the range within which sandy ～ muddy sediments are observed is extremely narrow. Rocks are mainly composed of autobrecciated lava but talus breccias are prominent on the southern crest part. Pillow lava is recognized, though rarely, among talus breccias. Sandy ～ muddy sediments are distributed over rocks. As rocks are often outcropped from beneath the sediments, the thickness of the sediments are considered to be relatively thin. Ripple marks are rarely identified on the surface of sediments.

No apparent sign of mineralizarion is identified on this track line.

Living things observed on this track line include echinoderms such as crinoids, asteroids, echinoids and holothurians, coelenterates such as actiniae, and fishes,

shrimps and crabs. Trace fossils are observed on the surface of sandy ~ muddy sediments.

<Track line 93SFDC06>

The location of the towing line, duration of observation and number of photographs taken are as follows:

Started at	: 21:29 on Oct. 5, 1993 (GMT)
Finished at	: 00:41 on Oct. 5, 1993 (GMT)
Starting point	: 8° 59.62'S·156° 11.00'E
Terminal point	: 9° 00.51'S·156° 14.61'E
Towed azimuth	: 104°
Distance observed	: 3.5 miles
Water depths observed	: between 2,176 m and 2,760 m
Duration of observation	: 3 hours and 12 minutes
Number of photographs taken	: 112 points

The observation was carried out roughly in the azimuth of W ~ E from the ridge's western slope of the seamount located on the north side of the seafloor spreading center through its summit part to the ridge's eastern slope. The location of the track line is shown in Annexed Figure 3(6) and the route map is shown in Annexed Figure 4(6).

Outcropped rock is prominent on this track line and the range within which sandy ~ muddy sediments are observed is narrow. The sandy ~ muddy sediments assume dark colors. They are distributed over rocks. As rocks are often outcropped from beneath the sediments, the thickness of the sediments appears to be thin. Ripple marks are observed on the sediments. Pillow lava is well developed on the western slope but slaggy lava and talus breccias are distributed from the marginal part of the western top to the eastern slope. The pillow lava presents the form of pillows or tubes. The average diameter of the pillow lava is between 1 m and 2 m. The surface structure of the slaggy lava is vesicular and coarse-grained. The morphology of the slaggy lava is irregular.

No apparent sign of mineralization is identified on this track line.

Living things observed on this track line include echinoderms such as holothurians, crinoids and hydrozoas, and fishes, shrimps and sponges. The sponges are living in flocks and sticking to rocks.

A number of holes with diameters of several centimeters and white spots with diameters of about ten centimeters appeared to be trace fossils are observed on the surface of the sandy ～ muddy sediments.

<Track line 93SFDC07>

The location of the towing line, duration of observation and number of photographs taken are as follows:

Started at	: 02:53 on Oct. 6, 1993 (GMT)
Finished at	: 05:55 on Oct. 6, 1993 (GMT)
Starting point	: 9° 03.39'S･156° 14.34'E
Terminal point	: 9° 04.13'S･156° 17.29'E
Towed azimuth	: 103°
Distance observed	: 3.1 miles
Water depths observed	: between 2,097 m and 2,911 m
Duration of observation	: 3 hours and 2 minutes
Number of photographs taken	: 104 points

The observation was carried out roughly in the azimuth of W ～ E from the western slope of the seamount lying on the north side of the seafloor spreading center (the seamount on the south side of the track line 93SFDC06) through its top to the eastern slope of the ridge. The location of the track line is shown in Annexed Figure 3(7) and the route map is shown in Annexed Figure 4(7).

Outcropped rock is prominent on this track line. Sandy ～ muddy sediments are seen only on the terrace part of the eastern slope and on the top. Sandy ～ muddy sediments assume dark brown. They are distributed over rocks. As rocks are often outcropped from beneath the sediments, the thickness of the sediments appear to be relatively thin. Ripple marks are observed on the surface of the sediments. Rocks are mainly composed of pillow lava (in the shapes of a pillow and a tube), and slaggy lava and talus breccias are observed locally.

Oxidized and altered brown precipitates are observed on this track line at 9° 03.8'S･156° 15.9'E (at the water depth of 2,124 m) for about two minutes' observation (for about 60 m).

Living things observed on this track line include echinoderms such as crinoids, hydrozoas, echinoids and holothurians, and fishes and shrimps.

Trace fossils are observed on the surface of the sandy ～ muddy sediments.

<Track line 93SFDC08>

The location of the towing line, duration of observation and number of photographs taken are as follows:

Started at	: 21:57 on Oct. 6, 1993 (GMT)
Finished at	: 01:16 on Oct. 7, 1993 (GMT)
Starting point	: 9° 18.72'S·156° 15.51'E
Terminal point	: 9° 18.72'S·156° 18.99'E
Towed azimuth	: 90°
Distance observed	: 3.1 miles
Water depths observed	: between 2,608 m and 3,138 m
Duration of observation	: 3 hours and 19 minutes
Number of photographs taken	: 112 points

The observation was carried out in the azimuth of W ~ E from the western slope of the seamount lying on the south side of the seafloor spreading center to the top of the seamount. The location of the track line is shown in Annexed Figure 3(8) and the route map is shown in Annexed Figure 4(8).

Outcropped rock is relatively prominent on this track line. The range within which sandy ~ muddy sediments are observed is relatively narrow. Slaggy lava is prominently distributed on the western slope and a gradual transition from talus breccias to pillow lava is observed on the top. The pillow lava presents a pillow shape with average diameters from 1 m to 2 m. The sediments assume light brown and ripple marks are commonly observed on their surface.

The evidence of indicating an apparent sign of mineralization is not identified.

Living things observed on this track line include echinoderms such as echinoids and holothurians, coelenterates such as actiniae, and fishes, shrimps and sponges. *Munidopsis sp.* of smaller than 5 cm are observed on the talus breccias in the vicinity of 9° 18.7'S·156° 18.2'E.

Trace fossils are identified on the surface of the sandy ~ muddy sediments.

<Track line 93SFDC09>

The location of the towing line, duration of observation and number of photographs taken are as follows:

Started at	: 03:47 on Oct. 7, 1993 (GMT)
Finished at	: 06:41 on Oct. 7, 1993 (GMT)